

## Quantum Rolling Friction

F. Intravaia<sup>1</sup>, M. Oelschläger<sup>2</sup>, D. Reiche<sup>2</sup>, D. A. R. Dalvit<sup>3</sup>, and K. Busch<sup>1,2</sup>

<sup>1</sup>*Humboldt-Universität zu Berlin, Institut für Physik, AG Theoretische Optik & Photonik, 12489 Berlin, Germany*

<sup>2</sup>*Max-Born-Institut, 12489 Berlin, Germany*

<sup>3</sup>*Theoretical Division, MS B213, Los Alamos National Laboratory, Los Alamos, New Mexico 87545, USA*



(Received 30 January 2019; published 17 September 2019)

An atom moving in a vacuum at constant velocity and parallel to a surface experiences a frictional force induced by the dissipative interaction with the quantum fluctuations of the electromagnetic field. We show that the combination of nonequilibrium dynamics, the anomalous Doppler effect, and spin-momentum locking of light mediates an intriguing interplay between the atom's translational and rotational motion. In turn, this deeply affects the drag force in a way that is reminiscent of classical rolling friction. Our fully non-Markovian and nonequilibrium description reveals counterintuitive features characterizing the atom's velocity-dependent rotational dynamics. These results prompt interesting directions for tuning the interaction and for investigating nonequilibrium dynamics as well as the properties of confined light.

DOI: [10.1103/PhysRevLett.123.120401](https://doi.org/10.1103/PhysRevLett.123.120401)

Quantum light-matter interactions continue to fascinate with intriguing and nonintuitive phenomena. During the last years, many interesting results involving nonequilibrium physics and light confinement in photonic and plasmonic systems have been reported. Although systems out of equilibrium are very common in nature, only recently have intense investigations started to unravel their relevance for both fundamental and applied research [1,2]. On the other hand, light confinement is already known for inducing several important behaviors. Nonetheless, it continues to surprise and is currently attracting attention, for instance, for conveying spin-orbit interactions of light (a.k.a. spin-momentum locking) [3–5]. Here, we combine these fields of research within a larger framework: We show that, when an atom is forced to move parallel to a surface, quantum rolling frictional dynamics results from the nonequilibrium interplay of the atomic translational and rotational motion. Despite the apparent resemblance to the behavior of a classical body rolling on a surface, the underlying physics of this phenomenon features many interesting counterintuitive aspects.

Because of quantum fluctuations, light-matter interactions lead to the occurrence of nonconservative (frictional) forces on electrically neutral and nonmagnetic objects [6,7]. These forces are quantum in nature and the physics behind quantum friction is related to the quantum Cherenkov effect through the anomalous Doppler effect [8–11]. In this process, real photons are extracted from the vacuum at the cost of the object's kinetic energy; they are absorbed and reemitted, thus producing a fluctuating momentum recoil [12]. When only the atomic translational motion is considered, spin-zero photons are absorbed and reemitted, and a net quantum frictional force that opposes the translational motion appears. This anisotropic process was investigated in many scenarios during the

last decade [6,13–20] and its connection to nonequilibrium physics was recently highlighted [21]. In this Letter we show that, when the rotational degrees of freedom are involved in the dynamics, the atom can also exchange angular momentum, absorbing and emitting photons with nonzero spin. However, due to nonequilibrium physics, the anomalous-Doppler effect and the spin-momentum locking of light [3–5], this stochastic process is peculiarly unbalanced: A force in the direction of the motion appears and partially compensates the translational friction. As a result, a net atomic rotation emerges with a sense opposite to that of classical rolling.

We consider a system at zero temperature consisting of an atom propelled at constant height  $z_a > 0$  parallel to a flat surface at  $z = 0$ . We focus on the nonequilibrium steady state (NESS) characterized by a constant velocity  $\mathbf{v}$  reached by the system when friction balances the external drive. In the NESS the frictional force can be written as  $\mathbf{F} = \mathbf{F}^t + \mathbf{F}^r$  [22], where

$$\mathbf{F}^t = -2 \int_0^\infty d\omega \int \frac{d^2\mathbf{k}}{(2\pi)^2} \mathbf{k} \text{Tr}[\underline{\mathcal{S}}_R^T(-\omega_{\mathbf{k}}, \mathbf{v}) \cdot \underline{\mathcal{G}}_I^s(\mathbf{k}, z_a, \omega)], \quad (1a)$$

$$\mathbf{F}^r = -2 \int_0^\infty d\omega \int \frac{d^2\mathbf{k}}{(2\pi)^2} \mathbf{k} \text{Tr}[\underline{\mathcal{S}}_I^T(-\omega_{\mathbf{k}}, \mathbf{v}) \cdot \underline{\mathcal{G}}_R^{as}(\mathbf{k}, z_a, \omega)]. \quad (1b)$$

$\omega_{\mathbf{k}}^\pm = \omega \pm \mathbf{k} \cdot \mathbf{v}$  is the Doppler-shifted frequency of the vacuum field in the atom's comoving frame,  $\mathbf{k}$  is the component of the wave vector parallel to the surface, and  $\underline{\mathcal{G}}(\mathbf{k}, z_a, \omega)$  is the Fourier transform of the electromagnetic

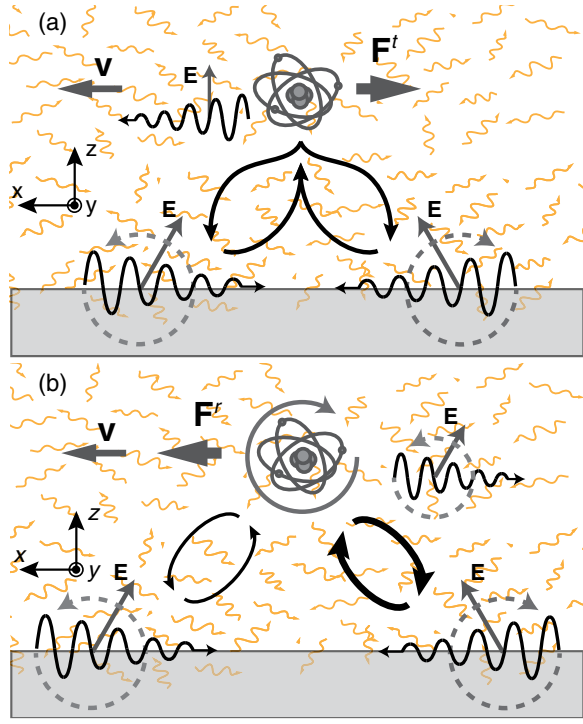


FIG. 1. Schematic description of the two mechanisms behind Eqs. (1). (a) In the near field two counterpropagating virtual surface excitations give rise to spin-zero photons (corresponding to a linearly polarized electromagnetic field  $\mathbf{E}$ ) that are absorbed by the atom, which gets excited (anomalous Doppler effect). The atom then emits linearly polarized photons, predominantly in the direction of the motion. The corresponding recoil momentum gives rise to  $\mathbf{F}^r$ . (b) When the atomic rotational degrees of freedom are involved in the dynamics, the atom can also absorb photons with nonzero spin (corresponding to circularly polarized electromagnetic field  $\mathbf{E}$ ). For a motion along the positive  $x$  axis, surface excitations with negative spin are predominantly absorbed, producing a clockwise rotation of the atom around the  $y$  axis. In this case, the atom prevalently emits photons with nonzero spin in the negative  $x$  direction, corresponding to the recoil force  $\mathbf{F}^r$  oriented in the direction of the motion.

Green tensor [22,23].  $\underline{S}(\omega, \mathbf{v})$  is the velocity-dependent atomic power spectrum, i.e., the Fourier transform of the stationary two-time correlation tensor  $\underline{C}_{ij}(\tau, \mathbf{v}) = \langle \hat{d}_i(\tau) \hat{d}_j(0) \rangle$  ( $i, j = x, y, z$ ). Here,  $\hat{\mathbf{d}}(t)$  describes the full nonequilibrium quantum dynamics of the particle's electric dipole vector operator. The symbol “Tr” traces over the Cartesian indices, while  $\mathsf{T}$  stands for the transpose. The superscripts  $s$  and  $as$ , and the subscripts  $R$  and  $I$  indicate the symmetric and the antisymmetric parts of tensors and the real and the imaginary part of the corresponding quantity, respectively.

The two terms in Eqs. (1) correspond to two distinct physical mechanisms characterizing the system [see Fig. 1]. A first insight about their origin is provided by looking at the correlation tensor: If  $\underline{C}(\tau, \mathbf{v}) = \underline{C}^{\mathsf{T}}(\tau, \mathbf{v})$ ,  $\underline{S}(\omega, \mathbf{v})$  is necessarily real and symmetric, leading to  $\mathbf{F}^r \neq 0$

and  $\mathbf{F}^r = 0$  [21,24]. This condition is equivalent to  $\langle \hat{\mathbf{d}}(\tau) \times \hat{\mathbf{d}}(0) \rangle = 0$ , which implies that, on average, the atomic dipole cannot rotate, absorb, or emit any net angular momentum.  $\mathbf{F}^r$  is therefore the quantum frictional force commonly investigated in the literature, which only takes into account the atomic translational motion.  $\mathbf{F}^r$  thus represents an additional contribution which appears if the rotational atomic degrees of freedom are considered and is the main focus of this work.

In order to obtain a deeper understanding, it is useful to analyze the Green tensor of our system. Without loss of generality we consider a motion along the  $x$  direction ( $\mathbf{v} = v\mathbf{e}_x$ ,  $|\mathbf{e}_x| = 1$ ). The surface-related (scattering) part of  $\underline{G}(\mathbf{k}, z_a, \omega)$  can then be written as the sum of a diagonal and a skew-symmetric matrix,  $\underline{\sigma}(\mathbf{k}, z_a, \omega)$  and  $-\phi(\mathbf{k}, z_a, \omega)\underline{L}_y$ , respectively.  $\underline{L}_y$  is the  $y$  component of the usual Lie-algebra's basis for  $\mathfrak{so}(3)$  ( $[\underline{L}_i]_{jk} = -i\epsilon_{ijk}$ ) describing 3D rotations [25]. As we will see in detail below [see Eqs. (4)],  $\underline{G}(\mathbf{k}, z_a, \omega)$ , describing the system's electromagnetic response, and  $\underline{S}(\omega, \mathbf{v})$ , accounting for the atomic fluctuations, are in general physically connected. The link is provided by the matrix  $\underline{G}_{\mathfrak{S}}(\mathbf{k}, z_a, \omega) = [\underline{G}(\mathbf{k}, z_a, \omega) - \underline{G}^{\mathsf{T}}(\mathbf{k}, z_a, \omega)]/(2i) = \underline{G}_I^s(\mathbf{k}, z_a, \omega) - i\underline{G}_R^{as}(\mathbf{k}, z_a, \omega)$ , which is related to the probability that the atom absorbs ( $\omega < 0$ ) or emits ( $\omega > 0$ ) photons [26]. With reference to the electromagnetic spin operator [4,5,27], the structure inherited from the Green tensor reveals that the interaction is sensitive to the three states of the photon's spin.  $\underline{G}_I^s(\mathbf{k}, z_a, \omega) = \underline{\sigma}_I(\mathbf{k}, z_a, \omega)$  is associated with linearly polarized photons (spin zero): Because of the matrix's even parity in  $\mathbf{k}$ , the corresponding processes do not depend on the direction of propagation. In contrast, the matrix  $\phi_I(\mathbf{k}, z_a, \omega)\underline{L}_y = \underline{G}_R^{as}(\mathbf{k}, z_a, \omega)$ , describes emission and/or absorption of photons having a nonzero spin along the  $y$  axis. The interpretation in terms of absorption and emission probability implies a positive spin when  $\phi_I < 0$  and a negative spin in the opposite case, linking the sign to the direction of propagation through the odd parity in  $\mathbf{k}$  of the function  $\phi$ . This locking behavior, which is essentially associated with the confinement of light at the vacuum-material interface [3–5], allows us to associate  $\phi_I(\mathbf{k}, z_a, \omega)$  with a spin-dependent local density of states. In the near-field limit we have [22,23]

$$\underline{G}(\mathbf{k}, z_a, \omega) \approx \underline{\Pi} \frac{k}{2\epsilon_0} r[\omega] e^{-2kz_a} \quad (k = |\mathbf{k}|), \quad (2a)$$

$$\underline{\Pi} = \begin{pmatrix} \frac{k_x^2}{k^2} & \frac{k_y k_x}{k^2} & -i \frac{k_x}{k} \\ \frac{k_y k_x}{k^2} & \frac{k_y^2}{k^2} & -i \frac{k_y}{k} \\ i \frac{k_x}{k} & i \frac{k_y}{k} & 1 \end{pmatrix} \rightarrow \begin{pmatrix} \frac{k_x^2}{k^2} & 0 & -i \frac{k_x}{k} \\ 0 & \frac{k_y^2}{k^2} & 0 \\ i \frac{k_x}{k} & 0 & 1 \end{pmatrix}. \quad (2b)$$

$\epsilon_0$  is the vacuum permittivity and  $r[\omega]$  the surface's  $p$ -polarized reflection coefficient. Please note, that in the

right-hand side expression we have deleted those terms that—due to symmetry—do not contribute to Eq. (1). As  $\underline{\Pi}^\dagger = \underline{\Pi}$ ,  $\underline{G}_\mathcal{S}$  is obtained by replacing  $r[\omega]$  with  $r_I[\omega]$  in Eq. (2a). At equilibrium and for common materials the radiation features zero angular momentum on average. However, for a moving atom, the frequency of the radiation in the comoving frame is Doppler shifted by the value  $\mathbf{k} \cdot \mathbf{v}$  [Eqs. (1)]. This induces an asymmetry in the spin balance and the atom effectively perceives spin-polarized radiation.

To quantitatively understand the implications of this phenomenon on the frictional force, we model the atom's internal structure as a Lorentz harmonic oscillator characterized by the transition frequency  $\omega_a$ . The velocity-dependent atomic polarizability tensor is then given by [21]

$$\underline{\alpha}(\omega, \mathbf{v}) = \alpha_B(\omega) \left( 1 - \alpha_B(\omega) \int \frac{d^2\mathbf{k}}{(2\pi)^2} \underline{G}(\mathbf{k}, z_a, \omega_{\mathbf{k}}^+) \right)^{-1}, \quad (3)$$

where  $\alpha_B(\omega) = \alpha_0 \omega_a^2 / (\omega_a^2 - \omega^2)$  and  $\alpha_0$  are the bare and static oscillator's polarizabilities, respectively. The non-equilibrium power spectrum can be written as

$$\underline{S}(\omega, \mathbf{v}) = \frac{\hbar}{\pi} [\theta(\omega) \underline{\alpha}_\mathcal{S}(\omega, \mathbf{v}) + \underline{J}(\omega, \mathbf{v})], \quad (4a)$$

where  $\underline{\alpha}_\mathcal{S}(\omega, \mathbf{v})$  is defined similarly to  $\underline{G}_\mathcal{S}(\mathbf{k}, z, \omega)$  and

$$\underline{J}(\omega, \mathbf{v}) = \int \frac{d^2\mathbf{k}}{(2\pi)^2} [\theta(\omega_{\mathbf{k}}^+) - \theta(\omega)] \times \underline{\alpha}(\omega, \mathbf{v}) \cdot \underline{G}_\mathcal{S}(\mathbf{k}, z_a, \omega_{\mathbf{k}}^+) \cdot \underline{\alpha}^\dagger(\omega, \mathbf{v}). \quad (4b)$$

The nonequilibrium fluctuation theorem in Eqs. (4) includes the atomic rotational degrees of freedom and generalizes results reported in previous work [21]. Equations (3) and (4) can be used to evaluate Eqs. (1). For illustration, we present the resulting frictional deceleration on a  $^{87}\text{Rb}$  atom moving above a gold surface in Fig. 2. For symmetry reasons the deceleration is along the direction of motion. Notice that the positive rotational contribution attenuates the frictional force stemming from the translation. Roughly speaking, one can say that, as in classical mechanics, allowing for a “rolling dynamics” reduces the frictional force acting on the object.

For additional insight and a more quantitative analysis, we focus on the low-velocity limit of Eqs. (1). As discussed in previous work [21,22,24], the dominant contribution to the frictional force arises from low frequencies  $\omega \lesssim v/z_a$ . If  $r_I \approx 2\epsilon_0\rho\omega$  for these frequencies (for conductors  $\rho$  is the resistivity) [21,30,31], to second order in  $\alpha_0$ , we have

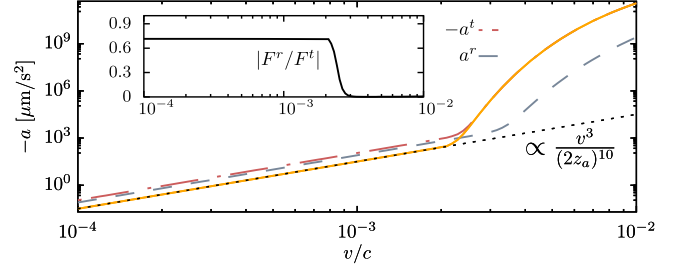


FIG. 2. Frictional acceleration,  $a = a^t + a^r$ , on a  $^{87}\text{Rb}$  atom ( $\alpha_0 = 4\pi\epsilon_0 \times 47.28 \text{ \AA}^3$ ,  $\omega_a = 1.3 \text{ eV}$ ,  $m_{\text{Rb}} = 86.9 \text{ u}$  [28]) as a function of its velocity. The particle moves at  $z_a = 5 \text{ nm}$  from a gold surface, described by a Drude permittivity  $\epsilon(\omega) = 1 - \omega_p^2 / [\omega(\omega + i\Gamma)]^{-1}$  ( $\omega_p = 9 \text{ eV}$ ,  $\Gamma = 35 \text{ meV}$  [29], giving  $\rho = \Gamma / [\epsilon_0 \omega_p^2] = 3.21 \times 10^{-8} \text{ } \Omega \text{ m}$ ). The two competing contributions  $a^t$  (dash-dotted line) and  $a^r$  (dashed line) in Eqs. (1) are represented. At small velocity the total acceleration (full line) scales as the sum of the expressions in Eq. (6) divided by the atomic mass (dotted line), while at high velocity friction is enhanced by a resonant interaction [21]. The inset shows that at low velocities  $F^r$  compensates more than 70% of  $F^t$ . The percentage decreases at higher velocity.

$$F^t \approx -\alpha_0^2 v^3 \frac{\hbar}{\pi} \int \frac{d^2\mathbf{k}}{(2\pi)^2} \frac{d^2\tilde{\mathbf{k}}}{(2\pi)^2} \frac{k_x}{6} (k_x + \tilde{k}_x)^3 \times \text{Tr}[\underline{\sigma}'_I(\mathbf{k}, z_a, 0) \cdot \underline{\sigma}'_I(\tilde{\mathbf{k}}, z_a, 0)], \quad (5a)$$

$$F^r \approx -\alpha_0^2 v^3 \frac{\hbar}{\pi} \int \frac{d^2\mathbf{k}}{(2\pi)^2} \frac{d^2\tilde{\mathbf{k}}}{(2\pi)^2} \frac{k_x}{6} (k_x + \tilde{k}_x)^3 \times \text{Tr}[\underline{L}_y^T \cdot \underline{L}_y] \phi'_I(\mathbf{k}, z_a, 0) \phi'_I(\tilde{\mathbf{k}}, z_a, 0), \quad (5b)$$

where the prime indicates the derivative with respect to the frequency. For a motion within the near field of the surface, Eqs. (5) give

$$F^t \approx -\frac{63}{\pi^3} \hbar \alpha_0^2 \rho^2 \frac{v^3}{(2z_a)^{10}}, \quad F^r \approx \frac{45}{\pi^3} \hbar \alpha_0^2 \rho^2 \frac{v^3}{(2z_a)^{10}}. \quad (6)$$

Notice that the contribution associated with the rotation compensates more than 70% of the force related to the translation (see inset in Fig. 2). Interestingly, one can show that at low velocity, using the so-called local thermal equilibrium (LTE) approximation, the compensation between the translational and the rotational contributions is complete, leading to an erroneous vanishing frictional force. The LTE approach is commonly used for an approximate description of nonequilibrium systems and treats each of its components as if they were locally in thermal equilibrium with their immediate surrounding. The (equilibrium) fluctuation-dissipation theorem (FDT) is then applied [32], which for our system is equivalent to neglecting  $\underline{J}$  in Eq. (4). A vanishing friction in the LTE approximation indicates that the detailed balance enforced by the FDT incorrectly treats the processes connected with

the translation and the rotation on the same footing. Contrasted with Eq. (6), the LTE result is not only flawed but also highlights that, as soon as the rotational degrees of freedom are included, quantum friction is essentially a pure nonequilibrium phenomenon.

The difference in sign between  $F^l$  and  $F^r$  can be understood as a consequence of the interplay between the anomalous Doppler effect and the spin-momentum locking of light. In the NESS, for a motion along  $x > 0$ , the Doppler-shifted frequency  $\omega_{\mathbf{k}}$  becomes “anomalously” negative only for  $k_x > 0$ . Therefore, during the motion the atom can get excited even at zero temperature [see the discussion before Eq. (2)] due to a light-matter interaction that favors positive  $k_x$ . In Eq. (5a) emission and absorption are controlled by  $\underline{\sigma}(\mathbf{k}, z_a, \omega)$  and involve spin-zero photons which are prevalently emitted in the direction of the motion. As a result, the net recoil force  $F^l$  acts against the motion [21,22,24]. However, allowing for the atomic rotational dynamics opens an additional channel of interaction with the surface represented by Eq. (1b). The corresponding processes in Eq. (5b) are associated with the product  $\phi(\mathbf{k}, z_a, \omega)\underline{L}_y$  and involve photons with nonzero spin. In this case, the angular momentum acts as an additional filter that selects a prevalent emission along the negative  $x$  direction. This leads to the net recoil force  $F^r$  with the same sign of the velocity.

The involvement of the angular momentum has an additional implication. During the motion and the interaction with the vacuum field, the atom undergoes a stochastic process which includes rotation. The stationarity characterizing the NESS implies that all torques acting on the atom, resulting from the dissipative nonequilibrium light-matter interaction, must balance on average. The rotational stochastic motion [33] generated by the exchange of photons can be associated with a constant angular momentum  $\mathcal{L} = [\alpha_0 \omega_a^2]^{-1} \langle \hat{\mathbf{d}}(t) \times \dot{\hat{\mathbf{d}}}(t) \rangle$ , which can be written as [34]

$$\mathcal{L} = \frac{1}{\alpha_0 \omega_a^2} \int_{-\infty}^{\infty} d\omega \omega \text{Tr}[\underline{L} \cdot \underline{S}(\omega, \mathbf{v})]. \quad (7)$$

In agreement with the symmetries of our system, only the  $y$  component is nonzero. We can evaluate the corresponding rotation frequency  $\Omega$  by multiplying the angular momentum by the inverse of the average atomic moment of inertia tensor,  $\underline{M}_{ij} = [\alpha_0 \omega_a^2]^{-1} \langle |\hat{\mathbf{d}}(t)|^2 \delta_{ij} - \hat{d}_i(t) \hat{d}_j(t) \rangle$ . With some matrix algebra this yields

$$\Omega = \frac{\int_{-\infty}^{\infty} d\omega \omega \text{Tr}[\underline{S}(\omega, \mathbf{v}) \cdot \underline{L}_y]}{\int_{-\infty}^{\infty} d\omega \text{Tr}[\underline{S}(\omega, \mathbf{v}) \cdot \underline{L}_y^2]}. \quad (8)$$

Inserting Eq. (4) in Eq. (8), in the near-field limit and for  $\omega_a$  within the Ohmic response of the material, we obtain at the leading order in  $\alpha_0$  [35]

$$\Omega \approx -\frac{v}{z_a} \left[ 1 + \left( \frac{1}{3} \frac{r_R[\omega_a]}{r_I[\omega_a]} \right)^2 \right]^{-1}. \quad (9)$$

Equation (9) indicates that, in the NESS, while propelled by a constant external force near the surface, translation and rotation couple and the atom rotates *clockwise* around the  $y$  axis despite no external torque is applied with respect to an axis passing through its center of mass (see Fig. 1). This last result contradicts our classical intuition, which, for a motion along the positive  $x$  axis, would instead suggest a counterclockwise rotation. It also differs from evaluations of purely rotating metallic nanoparticles without translational motion [36–39], or on immobile circularly polarized excited atoms [40] in front of a surface, which in the near-field and low rotational frequency limits predict lateral forces agreeing with the classical prescription. Once again, however, the sense of rotation can be interpreted as resulting from the motion-induced asymmetry in the light-matter interaction. In the atomic excitation process the anomalous Doppler effect favors the absorption of photons propagating along the positive  $x$  axis. In the near field they have negative spin, resulting in the absorption of negative angular momentum and a clockwise rotation of the atom. This also provides a better understanding of the sign of  $F^r$ : During the dissipative process associated with the frictional force, in order to keep  $\mathcal{L}$  constant, the atom emits photons with positive spin, thus absorbing a negative angular momentum recoil. Because of the properties of the spin-dependent density of states, in the near field these photons can be absorbed by the environment (essentially the surface) if they are emitted along the negative  $x$  axis, thus favoring a positive momentum recoil and a positive  $F^r$ . Still, because of the Doppler shift, the last process is less effective than the one associated with spin-zero photons, whose absorption rate does not depend on the sign of the wave vector, justifying why  $|F^r| < |F^l|$ .

It is important to highlight that our description takes into account the full nonequilibrium electromagnetic backaction on the microscopic object, setting it apart from other related studies. Nonequilibrium backaction is often not included in perturbative approaches for atoms [40,41] and it is commonly neglected for metallic nanoparticles [36,38,39], due to the strong intrinsic dissipation of the metal [22]. In our case, however, this feature ultimately characterizes important quantities such as the atomic power spectrum or polarizability and affects the spin-sensitive atom-surface interaction. Disregarding the backaction removes the intrinsic velocity dependence in these quantities, making them coincide with their bare or equilibrium expressions. This leads to a description which, to a large extent, is equivalent to the LTE approximation for which some of the above effects disappear.

The measurement of the quantum frictional force and of the corresponding deceleration is challenging due to the weakness of the interaction. It requires a careful choice of

both the experimental technique and the system's parameters. From Fig. 2, we see that on a rubidium atom moving at  $v \gtrsim 30$  km/s at a distance of 5 nm from a gold surface acts a deceleration  $|a| \gtrsim 3 \times 10^{-2} \mu\text{m/s}^2$ . Notice, however, that replacing  $^{87}\text{Rb}$  with  $^7\text{Li}$  ( $\alpha_0 = 4\pi\epsilon_0 \times 24.33 \text{ \AA}^3$  [42],  $m_{\text{Li}} = 7.02$  u) and gold with sodium ( $\rho = 8 \times 10^{-7} \Omega\text{m}$  [43]), already leads to a deceleration of  $2.5 \mu\text{m/s}^2$  for  $v \approx 10$  km/s. In addition, previous work has indicated that considering spatial dispersion and engineering the surface's optical response can enhance the effect by several orders of magnitude [30,31]. Consequently, promising perspectives for a detection are offered by atom interferometry. Cold-atom setups have already achieved an accuracy of  $10^{-2} \mu\text{m/s}^2$  [44] for the measurement of accelerations. To increase the (relative) velocity, one can consider atoms moving close to or trapped in a ring-shaped potential [45] parallel to a surface rotating with high frequency ( $v \sim 10$  km/s are reached in microturbines). Alternatively,  $v \gtrsim 100$  km/s are achieved using neutralized ion beams [46]. In this last case, one can search for friction-induced modifications of the interference pattern produced by the diffraction of the atomic beam on a grating with very small apertures ( $\sim 45\text{--}50$  nm [47–49]). An indirect proof for  $F^r$  can be provided by the detection of the atomic rotation. Using the parameters of Fig. 2, for  $v \approx 10$  km/s we obtain  $|\Omega| \approx 25$  MHz, which can be detected by measuring the atomic optical response to circular polarized light.

In conclusion, we have shown that the combination of nonequilibrium dynamics, the anomalous Doppler effect and the spin-momentum locking of light induces quantum rolling friction on an atom moving parallel to a surface. During the zero-temperature dissipative process, the atom performs a driven Brownian-like motion that involves its internal degrees of freedom and depends on the three states of the photon's spin. The atom absorbs and emits photons, exchanging translational and angular momentum with light. As in classical rolling motion, the interplay between atomic translational and rotational motion sensibly diminishes the drag force with respect to the case where the rotation is not considered. Interestingly, however, the reduction in strength of friction is connected with a steady atomic rotation with a sense opposite to what one would expect from classical intuition. Our analysis qualitatively applies to a large class of systems and materials showing similar features (low-frequency dissipation, light confinement, etc.). It also suggests ways for tuning the total quantum frictional interaction via an enhancement of the system's asymmetry. They can involve, for instance, chiral atoms [50], topological materials [51], or even external fields [52], which can affect the exchange of angular momentum within the system. Quantum rolling friction yields an interesting example on how different phenomena unconventionally combine in the quantum realm.

We thank R. O. Behunin, A. Manjavacas, P. Schneeweiss, A. Rauschenbeutel, and R. Decca for insightful discussions.

We acknowledge funding by the Deutsche Forschungsgemeinschaft (DFG) through SFB 951 HIOS (B10, Project No. 182087777) and by the LANL LDRD program. F. I. further acknowledges financial support from the DFG through the DIP program (Grants FO 703/2-1 and SCHM 1049/7-1).

- 
- [1] M. Esposito, U. Harbola, and S. Mukamel, Nonequilibrium fluctuations, fluctuation theorems, and counting statistics in quantum systems, *Rev. Mod. Phys.* **81**, 1665 (2009).
  - [2] A. Polkovnikov, K. Sengupta, A. Silva, and M. Vengalattore, Colloquium : Nonequilibrium dynamics of closed interacting quantum systems, *Rev. Mod. Phys.* **83**, 863 (2011).
  - [3] P. Lodahl, S. Mahmoodian, S. Stobbe, A. Rauschenbeutel, P. Schneeweiss, J. Volz, H. Pichler, and P. Zoller, Chiral quantum optics, *Nature (London)* **541**, 473 (2017).
  - [4] A. Aiello, P. Banzer, M. Neugebauer, and G. Leuchs, From transverse angular momentum to photonic wheels, *Nat. Photonics* **9**, 789 (2015).
  - [5] K. Y. Bliokh, F. J. Rodríguez-Fortuño, F. Nori, and A. V. Zayats, Spinorbit interactions of light, *Nat. Photonics* **9**, 796 (2015).
  - [6] G. Dedkov and A. Kyasov, Electromagnetic and electrodynamic forces of interaction of moving particles and nanoprobe with surfaces: A nonrelativistic consideration, *Phys. Solid State* **44**, 1809 (2002).
  - [7] A. I. Volokitin and B. N. J. Persson, Dissipative van der Waals interaction between a small particle and a metal surface, *Phys. Rev. B* **65**, 115419 (2002).
  - [8] V. Frolov and V. Ginzburg, Excitation and radiation of an accelerated detector and anomalous Doppler effect, *Phys. Lett. A* **116**, 423 (1986).
  - [9] M. V. Nezlin, Negative-energy waves and the anomalous Doppler effect, *Sov. Phys. Usp.* **19**, 946 (1976).
  - [10] V. L. Ginzburg, Radiation by uniformly moving sources (Vavilov–Cherenkov effect, transition radiation, and other phenomena), *Phys. Usp.* **39**, 973 (1996).
  - [11] M. F. Maghrebi, R. Golestanian, and M. Kardar, Quantum Cherenkov radiation and noncontact friction, *Phys. Rev. A* **88**, 042509 (2013).
  - [12] F. Intravaia, V. E. Mkrtchian, S. Y. Buhmann, S. Scheel, D. A. R. Dalvit, and C. Henkel, Friction forces on atoms after acceleration, *J. Phys. Condens. Matter* **27**, 214020 (2015).
  - [13] G. Barton, On van der Waals friction. II: Between atom and half-space, *New J. Phys.* **12**, 113045 (2010).
  - [14] M. G. Silveirinha and S. I. Maslovski, Exchange of momentum between moving matter induced by the zero-point fluctuations of the electromagnetic field, *Phys. Rev. A* **86**, 042118 (2012).
  - [15] G. Pieplow and C. Henkel, Fully covariant radiation force on a polarizable particle, *New J. Phys.* **15**, 023027 (2013).
  - [16] U. D. Jentschura, G. Lach, M. De Kieviet, and K. Pachucki, One-Loop Dominance in the Imaginary Part of the Polarizability: Application to Blackbody and Noncontact van der Waals Friction, *Phys. Rev. Lett.* **114**, 043001 (2015).
  - [17] J. Klatt, R. Bennett, and S. Y. Buhmann, Spectroscopic signatures of quantum friction, *Phys. Rev. A* **94**, 063803 (2016).

- [18] A. I. Volokitin, Anomalous Doppler-effect singularities in radiative heat generation, interaction forces, and frictional torque for two rotating nanoparticles, *Phys. Rev. A* **96**, 012520 (2017).
- [19] F. C. Lombardo and P. I. Villar, Quantum friction imprints on the geometric phase of a moving atom in front of a dielectric plate, *J. Phys. Conf. Ser.* **880**, 012035 (2017).
- [20] P. Rodríguez-Lopez and E. Martín-Martínez, Casimir forces and quantum friction of finite-size atoms in relativistic trajectories, *Phys. Rev. A* **98**, 032507 (2018).
- [21] F. Intravaia, R. O. Behunin, C. Henkel, K. Busch, and D. A. R. Dalvit, Non-Markovianity in atom-surface dispersion forces, *Phys. Rev. A* **94**, 042114 (2016).
- [22] F. Intravaia, R. O. Behunin, C. Henkel, K. Busch, and D. A. R. Dalvit, Failure of Local Thermal Equilibrium in Quantum Friction, *Phys. Rev. Lett.* **117**, 100402 (2016).
- [23] J. M. Wylie and J. E. Sipe, Quantum electrodynamics near an interface. II, *Phys. Rev. A* **32**, 2030 (1985).
- [24] F. Intravaia, R. O. Behunin, and D. A. R. Dalvit, Quantum friction and fluctuation theorems, *Phys. Rev. A* **89**, 050101 (R) (2014).
- [25] The Green tensor can be written as the sum of a vacuum and a scattering part. While the former is related to the properties of the homogeneous vacuum, the latter is related to the optical response and the geometry of the surface. The scattering part is responsible of most of our results while the vacuum part can be normally neglected.
- [26] L. Novotny and B. Hecht, *Principles of Nano-Optics*, 1st ed. (Cambridge University Press, New York, 2006).
- [27] L. Mandel and E. Wolf, *Optical Coherence and Quantum Optics* (Cambridge University Press, New York, 1995).
- [28] D. A. Steck, Technical report, Oregon Center for Optics and Department of Physics, University of Oregon, <http://steck.us/alkalidata/>.
- [29] T. G. Dominique Barchiesi, Fitting the optical constants of gold, silver, chromium, titanium, and aluminum in the visible bandwidth, *J. Nanophoton.* **8**, 083097 (2014).
- [30] D. Reiche, D. A. R. Dalvit, K. Busch, and F. Intravaia, Spatial dispersion in atom-surface quantum friction, *Phys. Rev. B* **95**, 155448 (2017).
- [31] M. Oelschläger, K. Busch, and F. Intravaia, Nonequilibrium atom-surface interaction with lossy multilayer structures, *Phys. Rev. A* **97**, 062507 (2018).
- [32] H. B. Callen and T. A. Welton, Irreversibility and generalized noise, *Phys. Rev.* **83**, 34 (1951).
- [33] B. A. Stickler, B. Schriniski, and K. Hornberger, Rotational Friction and Dissipation of Quantum Rotors, *Phys. Rev. Lett.* **121**, 040401 (2018).
- [34] M. R. Dennis, Geometric interpretation of the three-dimensional coherence matrix for nonparaxial polarization, *J. Opt. A: Pure and Appl. Opt.* **6**, S26 (2004).
- [35] The appearance of the surfaces reflection coefficient  $r[\omega]$  in Eq. (9) can be associated with the anisotropy of our system along the  $z$  direction. The oscillator describing the atom is indeed no longer isotropic, due to the frequency shift induced by the Casimir-Polder interaction with the surface.
- [36] R. Zhao, A. Manjavacas, F. J. García de Abajo, and J. B. Pendry, Rotational Quantum Friction, *Phys. Rev. Lett.* **109**, 123604 (2012).
- [37] F. J. Rodríguez-Fortuño, N. Engheta, A. Martínez, and A. V. Zayats, Lateral forces on circularly polarizable particles near a surface, *Nat. Commun.* **6**, 8799 (2015).
- [38] A. Manjavacas, F. J. Rodríguez-Fortuño, F. J. García de Abajo, and A. V. Zayats, Lateral Casimir Force on a Rotating Particle near a Planar Surface, *Phys. Rev. Lett.* **118**, 133605 (2017).
- [39] G. V. Dedkov and A. A. Kyasov, Dynamics of a nanoparticle rotating in the near field of a heated solid surface, *Tech. Phys.* **62**, 1266 (2017).
- [40] R. R. Q. P. T. Oude Weernink, P. Barcellona, and S. Y. Buhmann, Lateral Casimir-Polder forces by breaking time-reversal symmetry, *Phys. Rev. A* **97**, 032507 (2018).
- [41] S. Scheel, S. Y. Buhmann, C. Clausen, and P. Schneeweiss, Directional spontaneous emission and lateral Casimir-Polder force on an atom close to a nanobeam, *Phys. Rev. A* **92**, 043819 (2015).
- [42] A. Miffre, M. Jacquy, M. Büchner, G. Tréneç, and J. Vigué, Measurement of the electric polarizability of lithium by atom interferometry, *Phys. Rev. A* **73**, 011603 (2006).
- [43] E. J. Zeman and G. C. Schatz, An accurate electromagnetic theory study of surface enhancement factors for silver, gold, copper, lithium, sodium, aluminum, gallium, indium, zinc, and cadmium, *J. Phys. Chem.* **91**, 634 (1987).
- [44] A. D. Cronin, J. Schmiedmayer, and D. E. Pritchard, Optics and interferometry with atoms and molecules, *Rev. Mod. Phys.* **81**, 1051 (2009).
- [45] P. Navez, S. Pandey, H. Mas, K. Poullos, T. Fernholz, and W. von Klitzing, Matter-wave interferometers using TAAAP rings, *New J. Phys.* **18**, 075014 (2016).
- [46] C. Brand, M. Debiassac, T. Susi, F. Aguilon, J. Kotakoski, P. Roncin, and M. Arndt, Coherent diffraction of hydrogen through the 246 pm lattice of graphene, *New J. Phys.* **21**, 033004 (2019).
- [47] J. D. Perreault, A. D. Cronin, and T. A. Savas, Using atomic diffraction of Na from material gratings to measure atom-surface interactions, *Phys. Rev. A* **71**, 053612 (2005).
- [48] C. Brand *et al.*, An atomically thin matter-wave beam-splitter, *Nat. Nanotechnol.* **10**, 845 (2015).
- [49] A similar approach was already used for observing the van der Waals/Casimir-Polder interaction. See, for example, K. Hornberger, S. Gerlich, P. Haslinger, S. Nimmrichter, and M. Arndt, Colloquium: Quantum interference of clusters and molecules, *Rev. Mod. Phys.* **84**, 157 (2012).
- [50] P. Barcellona, H. Safari, A. Salam, and S. Y. Buhmann, Enhanced Chiral Discriminatory van der Waals Interactions Mediated by Chiral Surfaces, *Phys. Rev. Lett.* **118**, 193401 (2017).
- [51] S. A. Hassani Gangaraj, G. W. Hanson, M. Antezza, and M. G. Silveirinha, Spontaneous lateral atomic recoil force close to a photonic topological material, *Phys. Rev. B* **97**, 201108 (2018).
- [52] T. K. Rebane, Three-dimensional anisotropic harmonic oscillator in a magnetic field, *Opt. Spectrosc.* **112**, 813 (2012).